Biomedical Research 2017; 28 (17): 7398-7403

ISSN 0970-938X
www.biomedres.info

Experimental study of applying shear wave elastography for examining effects of high intensity focused ultrasound ablation against subcutaneously implanted VX_2 tumors in rabbits.

Fei Chen[1], Sheng Li[2], Limei Wu[3], Jianzhong Zou[4], Shaodong Qiu[5], Quanshi Wang[1*]

[1]Nanfang PET Center, Nanfang Hospital, Southern Medical University, Guangzhou, PR China

[2]Department of Medical Imaging, Sun Yat-sen University Cancer Center, Guangzhou, PR China

[3]Department of Clinical Laboratory, the Twelfth People's Hospital of Guangzhou, Guangzhou, PR China

[4]College of Biomedical Engineering, Institute of Ultrasound Engineering in Medicine, Chongqing Key Laboratory of Biomedical Engineering, Chongqing Medical University, Chongqing, PR China

[5]Department of Ultrasound, the Second Affiliated Hospital of Guangzhou Medical University, Guangzhou, PR China

Abstract

The aims of this study were to investigate the feasibility of applying Shear Wave Elastography (SWE) to evaluate the effects of High Intensity Focused Ultrasound (HIFU) ablation on Subcutaneously Implanted VX_2 tumors in rabbits (R-SIVX_2). The tumor hardness in a total of 20 R-SIVX_2 models was measured at different time points using SWE following HIFU ablation treatment. In SWE images, the VX_2 tumor appeared to be a homogeneous blue, and the average tumor hardness (E_{mean}) was 10.48 ± 0.33 Kpa. Tumor hardness on D1 was the highest (E_{mean}=97.45 ± 23.08 Kpa), and decreased gradually over a 30 d period, with tumor hardness on D30 being similar to that on D0. The hardness uniformity (E_{SD}) in the Region of Interest (ROI) increased significantly as compared to before the ablation, indicating that HIFU ablation can cause acoustic environmental changes in the organizations of the ROI. There were significant differences among E_{min}, E_{mean}, E_{max} and E_{SD} at different time points (P=0.00). There was no significant difference in E_{min} (E_{mean}) between D0 and D30 (P<0.05), but there was a significant difference between D0/D30 and D1/D7/D14 (P<0.05). The E_{max} values among different time points showed statistical significance (P<0.05), but the difference in E_{SD} between D3/D7 and D0/D1/D14/D30 was statistically significant (P<0.05). In addition to 2D ultrasound and color flow signals, SWE can provide tissue hardness information when used for evaluating the efficacy of HIFU ablation, which can provide useful information for evaluating the effects of tumor ablation.

Keywords: Elastography, High intensity focused ultrasound (HIFU), Ultrasound.

Accepted on July 17, 2017

Introduction

High Intensity Focused Ultrasound (HIFU) ablates tumors by means of heat and cavitation. Previous studies have shown that HIFU is an effective treatment [1-3]. HIFU is a kind of non-invasive treatment method to thermal ablate tumor *via* increasing temperature in target region, and some imaging methods, including MRI, CT and ultrasound, are used to perform therapeutic effect evaluation. Ultrasound is often used as an important imaging method for evaluating the efficacy of HIFU, and Ultrasound Elastography (UE), a new method for determining tissue hardness, is currently used in examining diseases in the breasts, thyroid, liver, and other tissues [4-10]. HIFU-induced damages in the target zone mainly appear as nuclear fragmentation or condensation, protein denaturation, cell membrane ruptures, cell gap increases, or tissue edemas, which can all lead to changes in tissue hardness. The clinical applications of our previous studies have focused on HIFU tumor ablation and ultrasonic elastography [11,12]. However, the clinical application of ultrasound elastography following HIFU tumor ablation has been scarcely reported in the literature [13]. Ultrasonic elastography combines both (quasi) static elastography and Shear Wave Elastography (SWE). SWE has attracted more and more attention owing to its strong repeatability and advantages over the measurement of the absolute value of hardness of the Region of Interest (ROI). In this study, we applied SWE to evaluate the effects of HIFU ablation on subcutaneously implanted VX_2 tumor in rabbits (R-SIVX_2). The application of ultrasound elastography in monitoring HIFU ablation will provide more abundant imaging information for the evaluation of HIFU ablation.

Methods

Establishment of R-SIVX$_2$ model

A total of 21 New Zealand white rabbits, weighing 2.0-3.0 kg, were implanted with subcutaneous VX$_2$ tumors using the tissue-embedding method (the tumor-bearing rabbits were provided by the Animal Center of Sun Yat-sen University). R-SIVX$_2$ model was constructed according to Li et al. [14]. The VX$_2$ tumor tissue was initially implanted in the hind limb of the donor rabbits. Each rabbit was then given general anesthesia with 3.0% pentobarbital (1.0 mL/kg), through an indwelling catheter in the auricular vein, for harvesting the VX$_2$ tumor. The tumor mass was then minced into 1.0-3.0 mm^3 pieces with a pair of scissors. After the rabbits were treated with anesthesia, two 1.0 cm-deep tunnels were made bilaterally under the hind limb skin, and one or two 1.0 mm^3 pieces of VX$_2$ tumor tissue were injected into each tunnel. The incisions were closed with 3.0 sutures. After approximately 15 d, the tumors grew to approximately 1.0-2.0 cm in diameter, and the rabbits were made ready for use in the experiment. This study was carried out in strict accordance with the recommendations in the Guide for the Care and Use of Laboratory Animals of the National Institutes of Health. The animal use protocol has been reviewed and approved by the Institutional Animal Care and Use Committee (IACUC) of Southern Medical University.

Standards of successful R-SIVX$_2$ model: (1) A subcutaneous mass in the rabbit hind leg can be observed with the naked eye and palpitation reveals a solid mass; (2) Ultrasound reveals that the subcutaneous mass in the experimental rabbits is hypoechoic; (3) The subcutaneous mass of one rabbit was confirmed to be originated from VX$_2$ tumor cells by Haematoxylin and Eosin (H and E) staining.

HIFU ablation

Each tumor-bearing rabbit was fixed on the treatment table in the prone position, and after the chest/abdominal skin was contacted with the media. The SIVX$_2$ tumor was then localized using the ultrasound probe of a JC-200 HIFU instrument (Haifu Technology Co., Ltd. Chongqing, China). The tumor level was selected as the therapeutic level, and was then irradiated by HIFU using the point-radiation method. The irradiation parameters were: power 250 W, radiation time interval 10 s, each point was irradiated twice, and the time interval was 10 s. There was no gap among the radiation points, and the treatment used the point-line-plane-body combination method. According to the layer thickness (3 mm), layer space (3 mm), and tumor size, 2 to 3 treatment planes can completely cover the tumor. During radiation, the innermost layer of the tumor was first irradiated, followed by gradual scanning from the deepest to the most superficial layers to cover the whole tumor. Ultrasound was performed immediately following the treatment of each layer. If the position changed during the treatment, the head position was re-adjusted, and the treatment then continued. At the end of the treatment, ultrasound was repeated to observe the ablation effects.

SWE studies

An ultrafast Ultrasound (US) system (Aixplorer, SuperSonicImagine (SSI), Aix-en-Provence, France) was used with an L15-4 probe. The principles of SSI have been described elsewhere [15]. Briefly, a vibration force was generated from two consecutive, focused US beams at different depths with 5.0 mm spacing. Each focused beam consisted of a 150 µs burst at 8.0 MHz. Propagating shear waves were imaged at a high frame rate (up to 20,000 frames/s), and raw radiofrequency data was recorded. Using a speckle-tracking correlation technique, movies of the displacements in the tissues, induced *via* the shear wave, were calculated. Then, the shear wave velocity was automatically deduced using a time-of-flight algorithm. The elastic modulus was determined from the shear wave speed in locally homogeneous soft tissues.

SWE can provide four parameters, namely the minimum hardness (E_{min}), the average hardness (E_{mean}), the maximum hardness (E_{max}), and the standard deviation of the hardness of the interest region (E_{SD}) when measuring the hardness of the ROI. This study adopted the device-default plotting features, namely the maximum range of “red” was about 100 Kpa. When sampling, the R-SIVX$_2$ was set as the ROI, and the largest cross-sectional area of the transplanted tumor was selected for the centralization of the sampling frame, so that the sampling diameter was consistent with the short diameter of the tumor.

In the present study, SWE was performed to measure the hardness of R-SIVX$_2$ at different time points, namely before the HIFU ablation (D0), 1 d after the ablation (D1), 7 d after the ablation (D7), 14 d after the ablation (D14), and 30 d after the ablation (D30) so as to observe the effects of HIFU treatment.

Statistical analysis

The measurement data was expressed as $\bar{x} \pm s$, and SPSS21.0 (IBM Corporation, Armonk, New York, USA) was used for the ANOVA and Student-Newman-Keuls (SNK) multiple comparisons of the E_{min}, E_{mean}, E_{max}, and E_{SD} so as to analyze the difference of the hardness in the ROI at different time points, with $P<0.05$ considered as statistically significant.

Results

Establishment of R-SIVX$_2$

When the R-SIVX$_2$ model was ready for use (before HIFU), general US and SWE were performed, demonstrating homogeneous and hyperechoic-to-isoechoic echoes in the tumors without evidence of liquefaction or necrosis.

The Color Doppler Flow Imaging (CDFI) signals with arterial tracing were detected in and around the tumors (Figure 1).

The volumes of VX$_2$ tumors were calculated based on the modified ellipsoidal formula: tumor volume=(length × width^2) × 0.5 [16]. The average volume of the transplanted VX$_2$ tumors was 0.74 ± 0.34 cm^3.

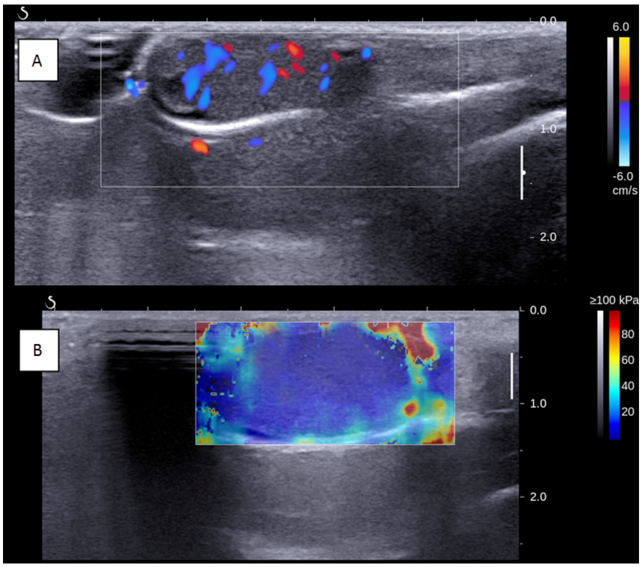

***Figure 1.** Ultrasonography of subcutaneously implanted VX_2 tumor in rabbits. (A) The lumps showed homogeneous low echo, and abundant blood flow signal could be seen in the interior and periphery; (B) SWE imaging, the tumor was relatively blue.*

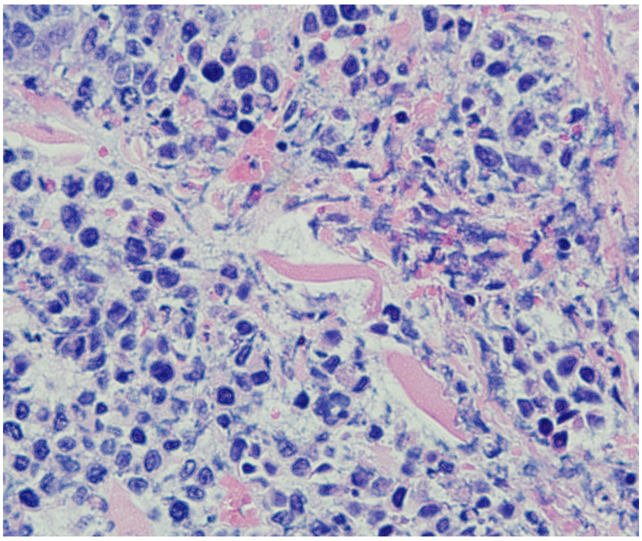

***Figure 2.** HE staining of subcutaneously implanted VX_2 tumor in rabbits (x40). HE staining showed that the tumor was originated from VX_2, and the tumor bearing rabbit model was successfully built.*

In the SWE images, the tumor appeared to be a uniform blue, with E_{mean} as 6.72 ± 0.38 Kpa, E_{mean} as 10.48 ± 0.33 Kpa, E_{max} as 14.67 ± 1.43 Kpa, and E_{SD} as 0.10 ± 0.003 Kpa.

One rabbit was then euthanized to verify the source of the subcutaneous mass. The H and E staining result is shown in Figure 2. The tumor cells were tightly arranged in a solid nest-like shape with large cells and rich cytoplasm. The cells were stained light red, the nuclei were large and pale, the nuclear membrane was clear, the chromatinic granules were coarse, the nuclear mitotic phases were common, and the intercellular fibrous connective tissues were less, confirming that the VX_2 was derived from the tumor.

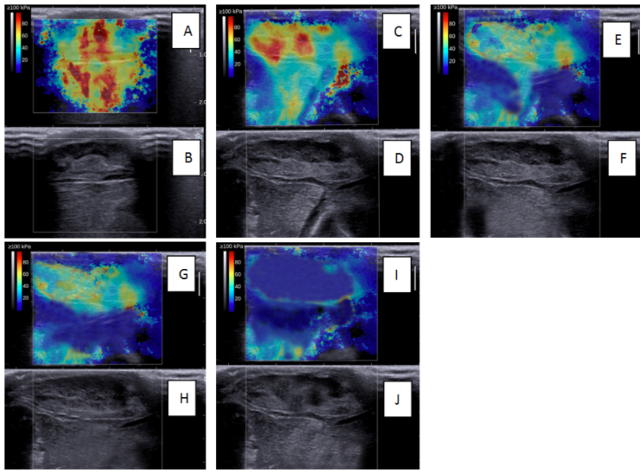

***Figure 3.** SWE ultrasound images at different time points after HIFU ablation. (A, B): 1 day after HIFU ablation, ablation zone of SWE ultrasound image was mainly red-yellow with colourful mosaic; (C, D): 3 d after HIFU ablation, the red area in ablation zone of SWE ultrasound images reduced; (E, F): 7 d after HIFU ablation, ablation zone of SWE ultrasound image was mainly blue-yellow; (G, H): 14 d after HIFU ablation, ablation zone of SWE ultrasound image was similar to those of 7 d after HIFU ablation; (I, J): 30 d after HIFU ablation, ablation zone of SWE ultrasound image was mainly blue, and partial liquefaction necrosis area could be seen in two dimensional ultrasonography.*

SWE observation of the effect of HIFU ablation

The SWE images obtained on D1-D30 revealed that the whole hardness of the ablation region exhibited a decreasing trend, and the tumor hardness on D30 was similar to that on D0. On D1, the tumor hardness in the ablation region and the surrounding region was increased significantly, and the E_{max} of the 20 masses measured reached 229.7 Kpa.

The region with hardness increased in SWE images was obviously larger than the mass region. The results of the E_{min}, E_{mean}, E_{max}, and E_{SD} at different time points are shown in Table 1.

Because one experimental rabbit was euthanized to verify the establishment of the R-SIVX_2 model, the number of rabbits observed at different time points was 20 (21-1=20). The SWE images at different time points are shown in Figure 3.

The ANOVA and SNK-t test for E_{min}, E_{mean}, E_{max}, and E_{SD} at the six time points (D0, D1, D3, D7, D14 and D30) showed that there were significant differences among the E_{min}, E_{mean}, E_{max}, and E_{SD} at different time points (P=0.00).

The multiple comparison results of the E_{min} and E_{mean} were similar: there was no statistical significance in the E_{max} (E_{mean}) between D0 and D30 (P>0.05), but the differences in the E_{max} (E_{mean}) between D0/D30 and D1/D7/D14 (P<0.05).

The E_{max} values among different time points showed no statistical significance (P<0.05), but the comparison of ESD between D3/D7 and D0/D1/D14/D30 was statistically significant (P<0.05).

Table 1. *Mass hardness measured by SWE at different time points (unit: kPa).*

	E_{min}	E_{mean}	E_{max}	E_{SD}
D0	6.72 ± 0.38	10.48 ± 0.33	14.67 ± 1.43	0.10 ± 0.003
D1	58.31 ± 19.95*	97.45 ± 23.08*	164.67 ± 47.31*	19.01 ± 8.22#
D3	45.77 ± 5.44*	68.17 ± 3.74#	94.98 ± 2.90#	14.39 ± 2.99*
D7	23.61 ± 3.89*	49.44 ± 5.29	76.57 ± 6.01	13.6 ± 2.20*
D14	34.34 ± 2.58*	40.72 ± 2.91	51.75 ± 4.61	8.22 ± 0.45
D30	5.87 ± 1.04	11.67 ± 1.76	31.97 ± 4.58□	4.44 ± 0.45□

*#□p<0.05.

Discussion

As a non-invasive treatment technique for tumors, HIFU has obtained wide and rapid clinical application in the past 20 y and has gradually become an effective method for anti-tumor therapy. Current imaging methods used for assessing the effects of HIFU ablation include ultrasound, computed tomography, or magnetic resonance imaging, but none of these methods can directly provide information regarding the basic mechanical properties of tissue hardness.

In 1991, Ophir et al. proposed the application of UE to quantitatively estimate and image the elastic modular distribution of the tissues [9]. Furthermore, the elasticity or hardness of biological tissues is largely dependent on the tissue molecules and micro and macro-organizational forms of such molecules, that is to say, when the tissue incurs pathological changes, its elasticity or hardness will also change. The pathological manifestations of the targeted HIFU ablation region mainly appear as nuclear fragmentation or shrinkage, cell lysis or melting, cell-structural destruction or disappearance, protein denaturation or tissue edema, which will lead to significant changes in tissue hardness [3]. If the effects of HIFU ablation can be followed up and evaluated based on the tissue hardness, it can provide important reference information. Therefore, elastography can provide meaningful reference information with regard to the status of the HIFU ablation region from a mechanical viewpoint.

Currently, UE techniques used in clinics mainly include (quasi) static elastic imaging technology and SWE. (Quasi) static elastic imaging is based on the deformation of the ROI caused by external pressure. Because elastic modulus are different among different tissues, their stains, caused by external or alternating vibration (mainly the morphological changes), are also different. Therefore collecting the signal fragments of the target during a certain time period, and analyzing these echo signals reflected before and after compression using the composite cross correlation method, can estimate the displacement of different tissue parts. This information can be used to calculate the deformation degrees of different tissues, which are then, imaged using a grayscale or color-coding method so as to demonstrate the hardness of the tissue in elastic images. Presently, (quasi) static elastic imaging technology is mainly used in examining diseases in the breasts, thyroid, and liver [17-20]. (Quasi) static elastic imaging technology has been applied in clinics previously, but this technology depends relatively heavily on the operator's skills and experience, therefore different operators often come to different results. Furthermore, this technology cannot reflect the absolute hardness of the tissue; therefore, SWE, which can measure the absolute tissue hardness, has become a new trend in clinical development.

SWE is a new method for obtaining elastographic images. Using this approach, an acoustic pressure wave induces slow-moving lateral waves within the tissue, and the speed of the shear wave propagation is proportional to the tissue's elastic modulus. Shear waves travel more slowly in softer tissues and more quickly in stiffer tissues. The ultrafast imaging of shear wave propagation allows for the measurement of the small changes in velocity that occur when the waves pass through tissues with different stiffness values. This velocity information can be mapped to create an image of the stiffness and provide quantitative elastic information in both kPa and m/s. SWE is less dependent on the operator, so more objective test results can be obtained. On the other hand, SWE can obtain the absolute hardness of the ROIs, and then label them with kPa or m/s, thus the measurement results are more accurate. At present, the clinical applications of SWE are mainly used in examining the liver, thyroid, and breasts [21,22].

In this study, we employed the R-SIVX_2 model through the tissue-embedding method, and then performed HIFU ablation. Before the ablation, we performed SWE and found that SWE can be used to examine the transplanted tumor, in which the hardness of the tumor was similar to that of surrounding soft tissues, and the hardness was relatively uniform. Among the four parameters used to reflect the ROI, E_{mean} reflects the average hardness of the ROI. On D1, the hardness of the mass was increased significantly. On one hand, through comparing the histological changes of the HIFU ablation zone in previous studies, this effect may have been due to such factors as some tumor cells beginning to dissolve after the ablation, and the neutrophils and lymphocytes beginning to infiltrate, or the tissues around the target zone were congested and bleeding. On the other hand, the increased area of the ROI was significantly greater than the tumor. This increase may have been caused by the micro-bubbles generated around the target zone due to the "cavitation effect" during the HIFU ablation process, which increases the acoustic reflection interface, thus increasing the speed of the shear waves and resulting in the increase of the hardness in the surrounding tissue mass [23]. With the reducing "cavitation effect", the hardness in the ablation and peripheral zones decreases; namely 3-7 d after the ablation, the hardness of the ablation zone, reflected by SWE, may be the more realistic tumor tissue hardness other than that affected by the "cavitation effect". In addition, as time goes on, the rupture, necrosis, and dissolution of tumor cells increases, and pathological changes occur, such as the infiltration of neutrophils and the proliferation of fibroblasts and fibrous connective tissue gradually appearing. Therefore, the mass's own hardness may still significantly increase compared with that before the ablation. In other words, the SWE images on D14 may better reflect the impact of HIFU ablation on the hardness of the tumor because the tissue hardness increases caused by the "cavitation effect" have essentially disappeared by this time, and SWE can then reflect the tumor hardness increases caused by the pathological changes. On D30, liquefaction necrosis occurs, thus affecting the mass's hardness, hence the E_{mean} value returned to the level consistent with the surrounding soft tissues. However, at this time, the E_{SD} value, which can reflect the uniformity degree of tissue hardness, was significantly increased as compared to before the ablation, indicating that the acoustic environment incurred significant changes after the ablation, and certain tissue components incurred significant differences as compared to those before the ablation.

Presently, although applying SWE for evaluating the effects of HIFU ablation has been preliminarily reported, this study applied SWE to observe the effects of HIFU ablation against R-SIVX$_2$ for the first time [24,25]. In addition to 2D ultrasound and blood flow signals, SWE can also provide tissue hardness data, and can show certain rules in the SWE images and shear wave velocity measurements targeting the ROI after HIFU ablation. Furthermore, such signs are closely related to the pathological changes and the tissue acoustic environment changes of the ROI after HIFU ablation. Therefore, we have reason to believe that application of SWE for evaluating the effects of HIFU ablation will have important clinical reference value.

Conflicts of Interest

All of the authors declare that they have no conflicts of interest regarding this paper.

References

1. Frulio N, Trillaud H, Perez P, Asselineau J, Vandenhende M, Hessamfar M, Bonnet F, Maire F, Delaune J, De Ledinghen V, Morlat P. Acoustic Radiation Force Impulse (ARFI) and Transient Elastography (TE) for evaluation of liver fibrosis in HIV-HCV co-infected patients. BMC Infect Dis 2014; 14: 405.
2. Zeng B, Chen F, Qiu S, Luo Y, Zhu Z, Chen R, Mao L. Application of quasistatic ultrasound elastography for examination of scrotal lesions. J Ultrasound Med 2016; 35: 253-261.
3. Wang HL, Zhang S, Xin XJ, Zhao LH, Li CX, Mu JL, Wei XQ. Application of real-time ultrasound elastography in diagnosing benign and malignant thyroid solid nodules. Cancer Biol Med 2012; 9: 124-127.
4. Matsubayashi RN, Imanishi M, Nakagawa S, Takahashi R, Akashi M, Momosaki S, Muranaka T. Breast ultrasound elastography and magnetic resonance imaging of fibrotic changes of breast disease: correlations between elastography findings and pathologic and short Tau inversion recovery imaging results, including the enhancement ratio and apparent diffusion coefficient. J Comput Assist Tomogr 2015; 39: 94-101.
5. Balu-Maestro C, Caramella T. Can breast elastography change our strategies? Technology, impact and limitations. Gynecol Obstet Fertil 2015; 43: 71-77.
6. Hong YR, Yan CX, Mo GQ, Luo ZY, Zhang Y, Wang Y, Huang PT. Conventional US, elastography, and contrast enhanced US features of papillary thyroid micro carcinoma predict central compartment lymph node metastases. Sci Rep 2015; 5: 7748.
7. Tomayko MM, Reynolds CP. Determination of subcutaneous tumor size in athymic (nude) mice. Cancer Chemother Pharmacol 1989; 24: 148-154.
8. Hirose T, Scheithauer BW, Lopes MB, VandenBerg SR. Dysembryoplastic neuroeptihelial tumor (DNT): an immunohistochemical and ultrastructural study. J Neuropathol Exp Neurol 1994; 53: 184-195.
9. Ophir J, Cespedes I, Ponnekanti H, Yazdi Y, Li X. Elastography: a quantitative method for imaging the elasticity of biological tissues. Ultrason Imaging 1991; 13: 111-134.
10. Maleke C, Konofagou EE. Harmonic motion imaging for focused ultrasound (HMIFU): a fully integrated technique for sonication and monitoring of thermal ablation in tissues. Phys Med Biol 2008; 53: 1773-1793.
11. Chenot J, Melodelima D, Souchon R, Chapelon JY. Hand-held Ultrasound Elastography for guiding liver ablations produced using a toroidal HIFU transducer. Res Animal Exp 2010; 383-386.
12. Orsi F, Zhang L, Arnone P, Orgera G, Bonomo G, Vigna PD, Monfardini L, Zhou K, Chen W, Wang Z, Veronesi U. High-intensity focused ultrasound ablation: effective and safe therapy for solid tumors in difficult locations. Am J Roentgenol 2010; 195: 245-252.
13. Zhang L, Zhu H, Jin C, Zhou K, Li K, Su H, Chen W, Bai J, Wang Z. High-intensity focused ultrasound (HIFU): effective and safe therapy for hepatocellular carcinoma adjacent to major hepatic veins. Eur Radiol 2009; 19: 437-445.
14. Li P, Zhu M, Xu Y, Zhao Y, Gao S, Liu Z, Gao YH. Impact of micro bubble enhanced, pulsed, and focused ultrasound on tumor circulation of subcutaneous VX2 cancer. Chin Med J 2014; 127: 2605-2611.
15. ter Haar G, Rivens I, Chen L, Riddler S. High intensity focused ultrasound for the treatment of rat tumours. Phys Med Biol 1991; 36: 1495-1501.
16. ter Haar G. High intensity focused ultrasound for the treatment of tumours. Echocardiography 2001; 36: 317-322.
17. Xiong X, Chen F, Chen J, Hsi R, Wu J, Zou J, He X. Pathologic evaluation of uterine fibroids ablated with high intensity focused ultrasound. Int J Clin Exp Pathol 2016; 9: 6163-6170.

18. Kim H, Kim JA, Son EJ, Youk JH. Quantitative assessment of shear-wave ultrasound elastography in thyroid nodules: diagnostic performance for predicting malignancy. Eur Radiol 2013; 23: 2532-2537.
19. Xia R, Thittai AK. Real-time monitoring of high-intensity focused ultrasound treatment using axial strain and axial-shear strain elastograms. Ultrasound Med Biol 2014; 40: 485-495.
20. Grajo JR, Barr RG. Strain elastography for prediction of breast cancer tumor grades. J Ultrasound Med 2014; 33: 129-134.
21. Ozmen E, Adaletli I, Kayadibi Y, Emre S, Kilic F, Dervisoglu S, Kurugoglu S, Senyuz OF. The impact of share wave elastography in differentiation of hepatic haemangioma from malignant liver tumors in paediatric population. Eur J Radiol 2014; 83: 1691-1697.
22. Miller DL, Song J. Tumor growth reduction and DNA transfer by cavitation-enhanced high-intensity focused ultrasound in vivo. Ultrasound Med Biol 2003; 29: 887-893.
23. Kwak JY, Kim EK. Ultrasound elastography for thyroid nodules: recent advances. Ultrasonography 2014; 33: 75-82.
24. Yan CX, Luo ZY, Liu XM, Huang PT, Mo GQ, Hong YR, Wen Q, Pan MQ, Weng HF. Ultrasonic scores of conventional ultrasound and ultrasound elastography in the diagnosis of thyroid nodular lesions. Zhonghua Yi Xue Za Zhi 2013; 93: 1630-1633.
25. Dudea M, Clichici S, Olteanu DE, Nagy A, Cucos M, Dudea S. Usefulness of real-time elastography strain ratio in the assessment of bile duct ligation-induced liver injury and the hepatoprotective effect of chitosan: an experimental animal study. Ultrasound Med Biol 2015; 41: 114-123.

*Correspondence to

Quanshi Wang

Nanfang PET Center

Nanfang Hospital

Southern Medical University

Guangzhou

PR China